Catalysis Letters Vol. 89, Nos. 1–2, July 2003 (© 2003)

A novel type of nanoporous carbon material supporting high dispersion of rhodium nanoparticles

Fengbo Li, Jin Zou, and Guoqing Yuan*

Institute of Chemistry, Chinese Academy of Sciences, Beijing, 100080, China

Received 21 February 2003; accepted 6 May 2003

Nanoporous carbon (NC) was prepared by the controlled pyrolysis of copolymer of vinylidene chloride and acrylonitrite. These organic–inorganic hybrid polymers were synthesized by suspending polymerization. After gradually controlled pyrolysis at 180–300 °C under nitrogen stream, the resulting material was carbonized at 1000 °C for 3 h under argon stream. In this way, nanoporous carbon was obtained, which has uniform pore size in the range of 0.8–1.6 nm and specific surface area of 900–1000 $m^2 g^{-1}$. The surface morphology and chemical composition were characterized by scanning electron microscopy (SEM) and X-ray photoelectron spectroscopy (XPS). Rhodium particles kept in a highly dispersed state over it were prepared and characterized by XPS and transmission electron microscopy (TEM). The expected high catalytic activity of the final material for methanol carbonylation was observed experimentally.

KEY WORDS: copolymer; carbonization; nanoporous carbon; supported metal; catalytic activity.

1. Introduction

Nanostructured carbon materials are potentially of great theoretical and technological importance for the development of catalysis [1,2]. Dispersion of metal particles determines the final catalyst activity and other properties [3]. Ordered nanoporous carbon made high dispersion of metal particles feasible, exceeding that of other common microporous carbon materials such as charcoal, activated carbon and carbon black [4]. The nanocasting process is the only route developed so far to produce ordered nanoporous carbon materials [4,5]. Here we describe an economical and easily operated strategy for obtaining a type of nanoporous material having uniform pore size in the range of 0.8–1.6 nm and specific surface area of 900–1000 $m^2 g^{-1}$. The final nanoporous material supports a high dispersion of rhodium nanoparticles, which are characterized by X-ray photoelectron spectroscopy (XPS) and transmission electron microscopy (TEM). High metal dispersion is an important design factor for the catalyst and is useful in practice, not only because it saves expensive metal but also because it controls structure sensitivity.

2. Experimental section

2.1. *Preparation of nanoporous carbon and supported rhodium nanoparticles*

Nanoporous carbon in this work is derived from organic–inorganic hybrid polymers, which are synthesized by suspending polymerization. Purified vinylidene chloride and acrylonitrile (2 : 1, mole ratio) were copolymerized in saturated Na_2SO_4 aqueous solution. The initiator was azobisisobutylvaleronitrile (ABVN) (1% (mole ratio) of monomers). Bentonite was used as the inorganic template and the dispersion phase. Copolymerization was kept at a constant temperature of 45 °C for 24 h, agitated with proper speed (200–250 r/min) in the first 12 h and then kept static. The polymeric materials were washed with hot water (80–95 °C) to remove excessive bentonite and purified in acetone stream to remove remaining monomers. The final copolymer was carbonized in a controlled manner to obtain ordered nanoporous carbon, heated at 180 °C for 12 h. Then the temperature was elevated to 300 °C by 1.0 °C min^{-1} and kept constant for 12 h, all in nitrogen stream. After removal of volatile molecules, the temperature was elevated from 300–1000 °C gradually and kept constant for 3 h in an argon stream. In this way, nanoporous carbon was obtained.

The precursor of rhodium nanoparticles was a binuclear rhodium carbonyl complex ($Rh_2Cl_2(CO)_4$), which was introduced by impregnating the nanoporous carbon in methanol solution of the complex for about 40 min, followed by drying in vacuum at ambient temperature. The dried fresh samples were reduced in a hydrogen stream at 400 °C for 75 min and then treated at experimentally designed temperature under an argon stream for 1 h. The metal loading was in the range of 1.0–1.2 wt%.

2.2. *Characterization of the resulting materials*

Prepared nanoporous carbons and supported rhodium were characterized by SEM, XPS and TEM. The

---

* To whom correspondence should be addressed.
E-mail: Yuangq@iccas.ac.cn

1011-372X/03/0700–0115/0

XPS measurement was carried out on an ESCA-Lab200I-XL (VG Science) spectrometer using Al Kα X-radiation at 15 kV × 20 mA, equipped with a hemispherical electron analyzer. All peak positions in XPS measurement were calibrated by the binding energy of C_{1s} at 284.6 eV as reference. Eclipse V2.1 data analysis software supplied by the manufacturer was used for manipulation of the acquired spectra. Specific surface area and pore size distribution were determined by an ST-03 apertometer. SEM was conducted on a Hitachi S530. Dispersion of supported metal particles was studied using a Hitachi H800 TEM operated at 100 kV.

3. Results and discussion

3.1. Surface properties of the prepared nanoporous carbon materials

The evolution of carbon structure and kinetics of carbonization will be discussed elsewhere. Here, our experimental observation and discussion focus on the surface chemical nature, pore size distribution and surface morphology.

The surface chemistry of carbon materials affects their behavior in practical application and is influenced to a large extent by the foreign elements fixed on the surface [6]. There are two types of heteroatoms in the

Table 1
The XPS analysis data of the resulting carbon

Index	Bonding energies (eV)	[AT] (%)		Chemical states
		573 K	1273 K	
C1s	283.62 ± 0.1	4.22	11.4	Silicon carbide
C1s	284.50 ± 0.1	32.2	39.6	Graphite carbon
C1s	285.08 ± 0.1	38.9	17.3	Amorphous carbon
C1s	286.18 ± 0.1	16.3	28.4	Carbon bonded with oxygen
C1s	289.02 ± 0.1	8.33	3.25	–CN, pyridine, shakeup satellites
N1s	399.01 ± 0.1	47.8	—	–CN (absorbed HCN)
N1s	398.60 ± 0.1	31.2	—	Pyridine
N1s	402.5 ± 0.1	21.0	—	$>N^{+}$–O

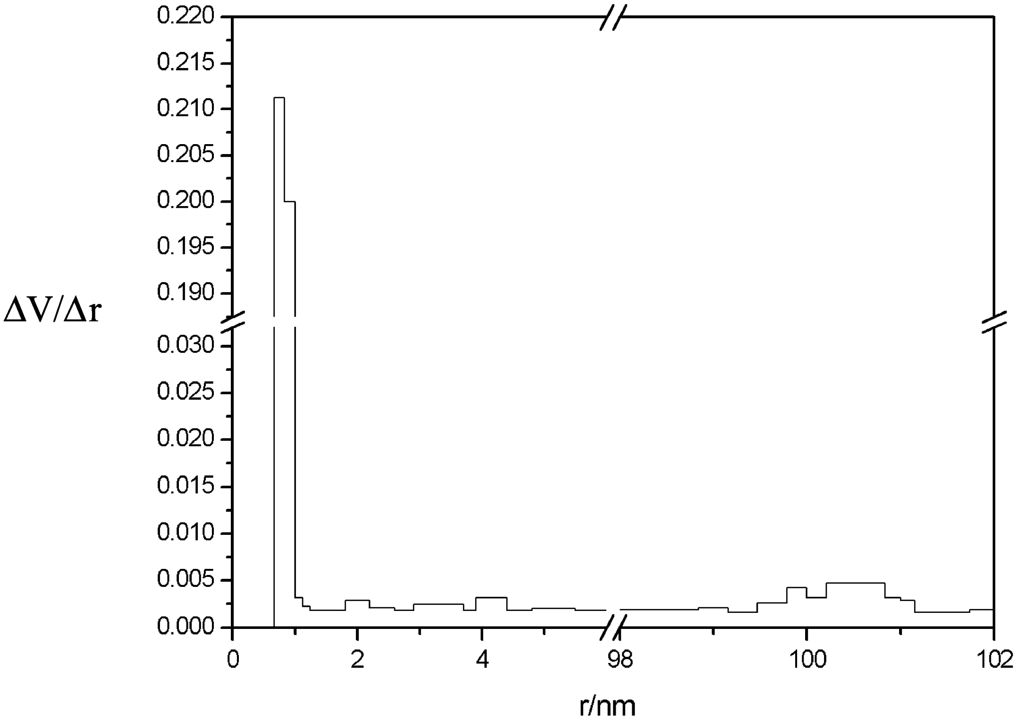

Figure 1. Pore size distribution of the prepared carbon ($\Delta V/\Delta r$ is the ratio of occupied pore volume to the range of pore size, r/nm is the pore size).

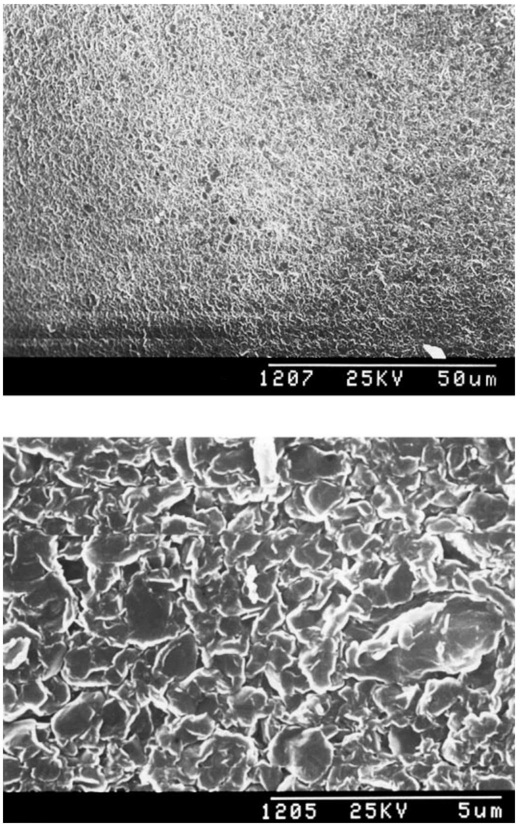

Figure 2. SEM images of the carbon material's surface at two different magnifications.

final materials as shown in table 1, which is mainly from bentonite. There were three types of heteroatoms (Si, O, N) in the materials treated at 300 °C, but when treated at 1000 °C, N was eliminated and the chemical state of Si and O changed. The XPS analysis data on the surface composition of the carbon are shown in table 1, the analysis reveals that more thermally stable oxygen surface groups occur on the prepared carbon surface. Clearly, the formation of more thermally stable oxygen surface groups has contributed to the increase in the atomic ratio bonding with oxygen.

Pore size distribution of the resulting carbon materials was determined by an ST-30 apertometer. Figure 1 presents the experimental observation that the size distribution is mainly in the range of 0.8–1.6 nm. Pore size is about 0.8–0.9 nm (inter pores); there are macropores (>100 nm) as well. Micropores contribute most to the high surface area of the carbon materials and provide high adsorptive capacities for the precursor molecules.

The contrast in SEM is due to the topography of the surface of the carbons. Figure 2 gives SEM images of the prepared carbons at two magnifications. Figure 2(a) is the low magnification view of the surface, showing uniform surface morphology and different form amorphous materials used as supports such as alumina, activated carbon and carbon black [7]. Figure 2(b) is a higher magnification view of the local surface, showing scale-like surface morphology.

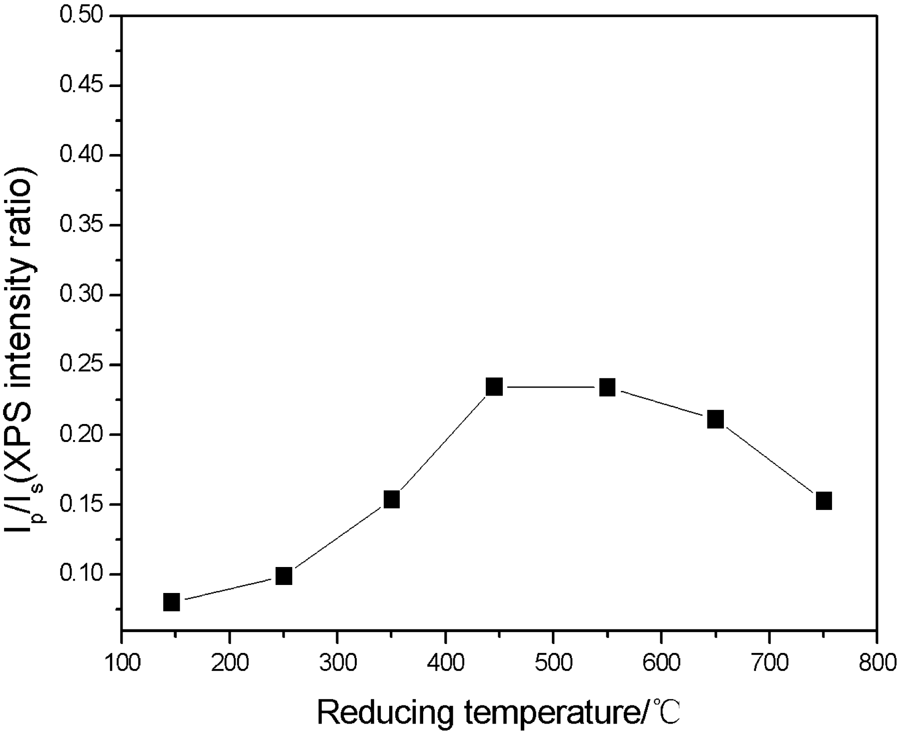

Figure 3. Variation of the XPS intensity ratio I_p/I_s (I_p is XPS intensity of the metal particles, I_s is XPS intensity of the support) on reduction temperature.

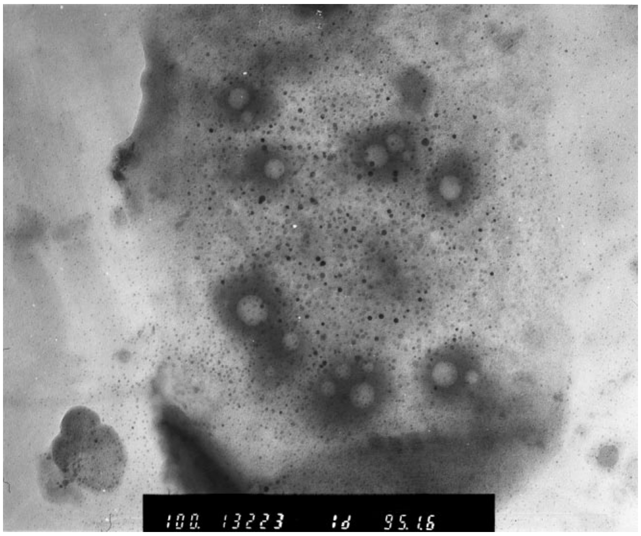

Figure 4. TEM image of the rhodium particles over the prepared carbon (black bar is scale bar/100 nm). Preparation conditions: metal loading 1.1 wt%, reduced at 400 °C in hydrogen for 75 min.

3.2. Characterization of supported rhodium particles

The XPS intensity ratio of the signals from the particles and the support, I_p/I_s, reflects the dispersion of the rhodium particles over the carbon support. Good dispersion leads to a high intensity ratio (I_p/I_s). If the metal loading is known, the XPS intensity ratio can be used to estimate the size of the metal particles [8,9]. Figure 3 gives the dependence of the XPS intensity ratio on reduction temperature (samples reduced for the same time). XPS intensity ratio attains a maximum at 450 °C, which is the proper reduction temperature for practical application. Figure 4 is a TEM image of the sample reduced by a hydrogen stream at 400 °C. This image clearly shows that Rh particles are mostly under 3 nm (black bar is scale bar/100 nm).

Table 2
Comparison of catalytic activity with the reported catalysts

Catalysts	Preparation and test conditions	Activity
Rh/Al_2O_3 [10]	Calcined in hydrogen at 573 K	No activity
Rh/Al_2O_3-SiO_2 [10]	Calcined in hydrogen at 573 K	No activity
Rh/SiO_2 [10]	Calcined in hydrogen at 573 K	No activity
Rh/BPL carbon [11]	1 wt% Rh, 208 °C, 16 atm, FBR, 20–30 mesh	64% (methanol conversion)
Rh/NC	1 wt% Rh, 180 °C, 10 atm, FBR, >40 mesh	81% (methanol conversion)

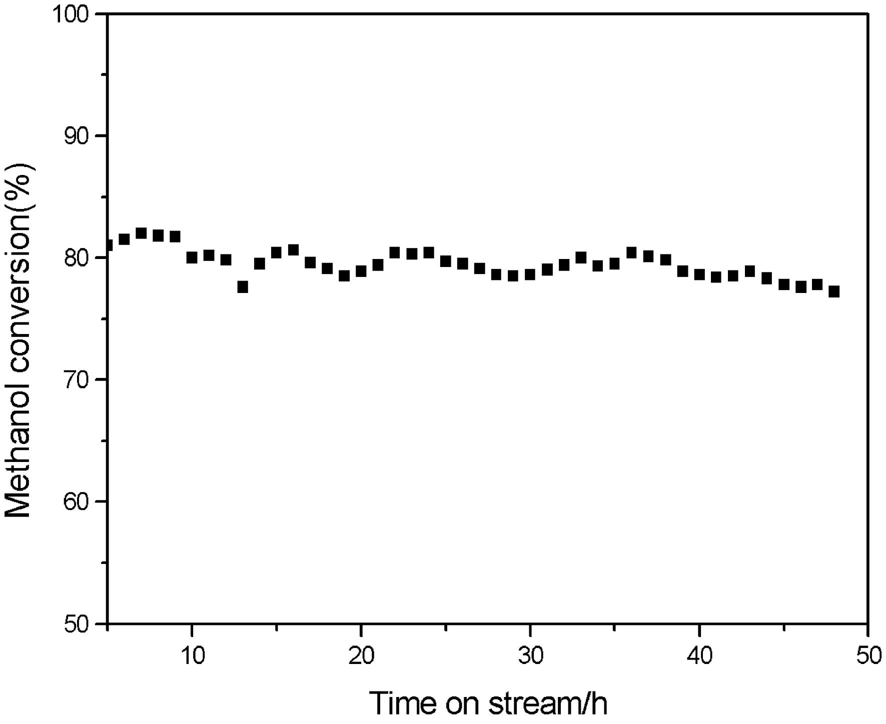

Figure 5. The stability of the resulting materials. Reaction conditions: metal loading 1.1 wt%, temperature 180–190 °C, total pressure 1.0 MPa, feed composition CO:MeI:MeOH = 80.1:1.94:17.96 (mole ratio).

3.3. Measurements of catalytic activity for methanol carbonylation

Methanol carbonylation in the presence of cocatalyst methyl iodide was chosen to assess the catalytic activity of the final materials. The catalytic test was conducted in a fixed-bed reactor. Table 2 compares the test results with reported supported Rh catalysts, which demonstrates that high dispersion of metal leads to high catalytic activity. Figure 5 gives the catalytic activity with time on feed gas stream. The fluctuations of activity are negligible and the catalyst shows good stability; with other supports such as activated carbon, carbon black and alumina, the catalysts were deactivated gradually, owing to metal loss (weak metal–support interaction) and sintering (low thermal stability) [13,14]. The experimental observation reveals that the resulting nanoporous carbon can stabilize the dispersed metal.

References

[1] J.M. Planeix *et al.*, J. Am. Chem. Soc. 116 (1994) 7935.
[2] N.M. Rodriguez, A. Chamer and R.T.K. Baker, Langmuir 11 (1995) 3862.
[3] A.Y. Stakheev and L.M. Kustov, Appl. Catal., A 188 (1999) 3.
[4] H.J. Sang, J.C. Secong *et al.*, Nature 412 (2001) 169.
[5] S. Ferdi, Chem. Mater. 13 (2001) 3184.
[6] H.P. Boehm, Carbon 32 (1994) 759.
[7] B.C. Cate, Chem. Rev. 75 (1995) 510.
[8] J.W. Niemantsverdriet, *Spectroscopy in Catalysis* (Wiley-VCH, 2000) p. 51.
[9] A. Frydman, D.G. Gastner, M. Schmal and C.T. Campbell, J. Catal. 157 (1995) 133.
[10] Y. Tatsuki, O. Yuichi, T. Nobuo and H. Nobuoyoshi, J. Catal. 59 (1979) 53.
[11] K.K. Robinson, A. Hershman, J.H. Carddock and J.F. Roth, J. Catal. 27 (1972) 389.
[12] H.B. Calin, Appl. Catal., A 212 (2001) 17.
[13] J.A. Moulijin, A.E.V. Diepen and F. Kapterjin, Appl. Catal., A 212 (2001) 3.